

To share and not share a singlet: quantum switch and nonclassicality in teleportation

Kornikar Sen,¹ Adithi Ajith,^{1,2} Saronath Halder,^{1,*} and Ujjwal Sen¹

¹Harish-Chandra Research Institute, A CI of Homi Bhabha National Institute, Chhatnag Road, Jhansi, Allahabad 211 019, India

²Indian Institute of Science, CV Raman Road, Bengaluru, Karnataka 560 012, India

The superposition principle provides us the opportunity to unfold many surprising facts. One such fact leads to the generation of entanglement which may allow one to teleport an unknown quantum state from one location to another. While all pure entangled states can provide nonclassical fidelity for quantum teleportation, perfect teleportation comes at the cost of having a maximally entangled state shared between the sender and the receiver. In this work, we consider a situation where the sender and the receiver are in a superposed situation of sharing a maximally entangled state and not sharing anything, controlled by a quantum switch. We consider two distinct protocols: in the first case, the sender and the receiver do nothing when there is no shared entanglement and in the second case, they use classical communication in absence of entanglement. In each of the protocols, we follow two different paths. In the first path, after the protocol is completed, we simply throw away the switch. In the second path, after accomplishing the protocol, we operate a Hadamard gate on the switch, measure the switch's state, and consider the outcome corresponding to a particular state of the switch. We compare the two paths with the maximum fidelity achievable through random guess or utilizing classical resources only. In particular, we provide conditions to achieve nonclassical fidelity in teleportation by applying quantum switch. We comment on whether the difference between the two paths can be expressed in terms of quantum coherence present in the switch's state.

I. INTRODUCTION

Quantum mechanics allows one to send the information of a quantum state without transporting the actual quantum system. This is possible due to the discovery of quantum teleportation by Bennett *et al.* [1]. After its introduction, quantum teleportation has received tremendous attention (for a review one can have a look into Ref. [2] and for other works, the references within that review). Apart from the communicational advantages, there exist various applications and variations of the teleportation protocol, some of which are remote state preparation [9], telecloning [10], etc [3, 4]. One remembers the protocol of entanglement swapping in this respect [5–8]. Teleportation has been experimentally realized using photonic systems shared over free space [11–16], ion traps [17, 18], nuclear magnetic resonances [19], superconducting circuits [20], optical fibers [21–23], etc.

To teleport an arbitrary quantum state perfectly, a maximally entangled state is needed to be shared between the sender and the receiver [24]. But in reality, the creation and preservation of maximally entangled states are very difficult. Instead of using a maximally entangled state if a less entangled state is used, it is possible to teleport a state which is *close* to the actual state, where the word ‘close’ is used in the sense of fidelity [25]. Thus, teleportation of a state by using a less-resourced state than maximally entangled has been a popular direction of research [26–31]. In absence of shared entanglement as well as the facility of classical communication, the receiver can just randomly prepare a state which will have the average fidelity $\frac{1}{2}$ to the actual state, in case of qubits. On the other hand, if the sender measures her/his qubit state,

classically informs the receiver about its outcome, and the receiver prepares that outcome in her/his lab, then the maximum fidelity that can be achieved is $\frac{2}{3}$ [32, 33]. Thus, fidelity larger than $\frac{2}{3}$ indicates quantum advantage for teleportation of qubits.

A quantum switch is a device which can be in superposition of two orthogonal physical situations, say $|on\rangle$ and $|off\rangle$, and correspondingly the transformation of a system may be controlled by the state of the switch. Effects of quantum switch have been explored in the context of indefinite causal orders [34–44]. Applications of quantum switches provide advantages in many quantum tasks, and for example, it helps to increase the precision of quantum metrology [41], diminishes complications of quantum communications [38, 39, 43, 45], etc. To explore experiments on quantum switches, see Refs. [46–50].

In [51], Jozsa dealt with a situation where a quantum computer is in a superposition of being switched on and off. It was shown that even in the limit that the quantum computer is almost completely off there is quantum advantage over the corresponding classical scenario. Recently, Siddiqui and Qureshi [52] have considered the double-slit experiment, which has its path detectors in a superposition of being present and absent and in that set-up, it was shown that the wave-particle duality relations are still valid. The concept of quantum switch has also been studied in the context of teleportation protocols [42, 53]. In [42], the authors have considered two teleportation channels in superposition of causal orders controlled by a quantum switch and have shown that even if noisy mixed states are used as resource, much higher fidelity can be achieved than the classical case. Applications of quantum switches in continuous-variable teleportations are discussed in [53].

In this paper, we introduce a quantum switch which controls the teleportation channel. The $|on\rangle$ state of the switch implies that a maximally entangled state is available and it is not available if the switch is in the $|off\rangle$ state. We consider

* Current Affiliation: Centre for Quantum Optical Technologies, Centre of New Technologies, University of Warsaw, Banacha 2c, 02-097 Warsaw, Poland

two different protocols separately in this context. In both protocols, when the switch is in $|\text{on}\rangle$ state, the usual teleportation protocol is performed, but when the switch is in $|\text{off}\rangle$ state, in the first protocol, the channel does nothing whereas, in the second protocol, the participants make use of classical communication. In each of the protocols, we consider two paths of the process. In the first path, after performing the protocols we just ignore the switch. In the second path, after the application of the protocols, we operate a Hadamard gate on the switch's state, measure the switch, and select a particular pre-decided outcome. We compare the protocols with classical protocols using the average fidelity of the received state with respect to the desired state. We observe that in the case of Protocol 1, Path 1 is guaranteed to provide more fidelity than the average fidelity of random guess, but in the case of Path 2, no such assurance can be offered. Similarly, in Protocol 2, Path 1 will always provide more fidelity than the maximum attainable fidelity using classical communication only, which is expected since in the second protocol the performers do make use of the classical communication. Again, the second path does not guarantee any such property. We also prove that the qualitative information about the advantage of one path over the other depends only on the phase between the $|\text{on}\rangle$ and $|\text{off}\rangle$ states and not on the probability amplitudes. Furthermore, we establish a relation between the advantage of using Path 2 over Path 1 and quantum coherence of the initial switch's state. It is proved that in a particular range of parameters, the advantage is a monotonically increasing function of quantum coherence of the switch, measured in the computational basis. Because of computational simplicity, we have analyzed single-qubit teleportation only, but the present idea can also be generalized to higher dimensions.

The rest of the paper is organized as follows: in Sec. II, we give a brief description of the standard teleportation protocol and about a small modification that we add. The exact scenario which we examine is introduced in Sec. III. The discussions and results of Protocol 1 are also presented in the same section. We move to Protocol 2 in the next section, i.e., in Sec. IV. The relation of quantum coherence with the difference between the fidelities corresponding to the two paths are explored in Sec. V. Finally, our concluding remarks are presented in Sec. VI.

II. PREREQUISITES

In a teleportation protocol, a sender, Alice, tries to teleport the state of an unknown qubit A' to a receiver, Bob, using local quantum operations and classical communication (LOCC) instead of physically sending the quantum system, but using pre-shared entanglement. Let the state of A' be $|\psi\rangle_{A'}$. As a resource of the protocol, Alice's lab contains another qubit, A , which is entangled with a qubit of Bob's lab denoted by B .

The exact teleportation of the state of A' requires the qubit-pair AB to be in a maximally entangled state, say the singlet, $|\psi^-\rangle_{AB} = \frac{1}{\sqrt{2}}(|01\rangle - |10\rangle)$. The steps of the actual protocol are described below:

1. Alice jointly measures the state $|\psi\rangle_{A'}$ and her part of the state $|\psi^-\rangle_{AB}$ in the Bell basis, $\{|\phi^+\rangle_{A'A}, |\phi^-\rangle_{A'A}, |\psi^+\rangle_{A'A}, |\psi^-\rangle_{A'A}\}$, where $|\phi^\pm\rangle_{A'A} = \frac{1}{\sqrt{2}}(|00\rangle \pm |11\rangle)$ and $|\psi^\pm\rangle_{A'A} = \frac{1}{\sqrt{2}}(|01\rangle \pm |10\rangle)$.
2. Using classical communication, Alice informs the output of her measurement to Bob.
3. Depending on the output, Bob applies one of the operators, $\{I_B, \sigma_x, \sigma_y, \sigma_z\}$ on his qubit. Here I_B denotes identity operator on the Hilbert space representing Bob's qubit and $\sigma_x, \sigma_y, \sigma_z$ are Pauli matrices acting on the same Hilbert space.

Along with the above steps from the original teleportation protocol, we add another step.

- Alice, at the end, applies one of the operators $\{I_A, \sigma_x, \sigma_y, \sigma_z\}$ on the qubit A , depending on the result of her measurement, to transform her two-qubit state into a singlet. Here the operators carry the same meaning as above, but defined to act on a qubit Hilbert space of Alice, viz. A , and for example, I_A is again an identity operator but acts on the Hilbert space of A .

The complete process of this teleportation protocol can be performed using the following Kraus operators:

$$\begin{aligned} K_1 &= (|\psi^-\rangle\langle\psi^-|)_{A'A} \otimes I_B, \\ K_2 &= (I_{A'} \otimes (\sigma_z)_A \otimes I_B)(|\psi^+\rangle\langle\psi^+|)_{A'A} \otimes (\sigma_z)_B, \\ K_3 &= (I_{A'} \otimes (\sigma_x)_A \otimes I_B)(|\phi^-\rangle\langle\phi^-|)_{A'A} \otimes (\sigma_x)_B, \\ K_4 &= (I_{A'} \otimes (\sigma_y)_A \otimes I_B)(|\phi^+\rangle\langle\phi^+|)_{A'A} \otimes (\sigma_y)_B, \end{aligned}$$

where $I_{A'}$ represents the identity operator acting on the qubit A' . The output state of the protocol is

$$\rho' = \sum_{\mu=1}^4 K_\mu \rho K_\mu^\dagger = (|\psi^-\rangle\langle\psi^-|)_{A'A} \otimes (|\psi\rangle\langle\psi|)_B,$$

where $\rho = (|\psi\rangle\langle\psi|)_{A'} \otimes (|\psi^-\rangle\langle\psi^-|)_{AB}$ is the density matrix representation of the initial state (before the teleportation protocol is performed). The operators, $K_\mu \forall \mu = 1, 2, 3, 4$, are defined in such a way that $K_\mu \rho K_\mu^\dagger = \frac{1}{4}(|\psi^-\rangle\langle\psi^-|)_{A'A} (|\psi\rangle\langle\psi|)_B \forall \mu$.

If instead of pursuing the teleportation protocol, Bob randomly guesses the state and creates it in his lab, then the average fidelity of the randomly generated state to the actual state is $\frac{1}{2}$. On the other hand, if the maximally entangled state is not available but utilization of the facility of classical communication is still possible, then the maximum average fidelity can be raised to $\frac{2}{3}$ [32, 33]. We want to compare our protocol with these fidelities, identifying them as classical scenarios.

III. NO CLASSICAL COMMUNICATION WHEN THE SWITCH IS OFF

In this section, we consider the situation where the actual teleportation protocol is controlled by a quantum switch. We

note here that whenever we consider a “switch” in this paper, we mean a quantum switch. We also note that ‘the switch is on’ means that the state of the quantum switch is $|\text{on}\rangle$ and ‘the switch is off’ means that the state of the quantum switch is $|\text{off}\rangle$. The switch indicates whether the singlet state (which is used as resource) is available or not. In particular, Alice’s lab contains another qubit (other than A and A'), which acts as the switch S . Bob’s lab contains only the single qubit, B . We now consider the following two physical situations:

$$|\text{on}\rangle_S |\psi\rangle_{A'} |\psi^-\rangle_{AB} \text{ and } |\text{off}\rangle_S |\psi\rangle_{A'} |\psi^-\rangle_{AB}.$$

When the switch is in the state $|\text{on}\rangle$, we follow the usual teleportation protocol. Thus, the state of the four qubits including the switch state transforms as

$$|\text{on}\rangle_S |\psi\rangle_{A'} |\psi^-\rangle_{AB} \rightarrow |\text{on}\rangle_S |\psi^-\rangle_{A'A} |\psi\rangle_B.$$

When the switch is in the state $|\text{off}\rangle$, we do nothing, and therefore, the qubits are left with what we had initially, viz. $|\text{off}\rangle_S |\psi\rangle_{A'} |\psi^-\rangle_{AB}$. In this case, the parties do not even use classical communication. We refer to this as **Protocol 1**. This process can be implemented using the following Kraus operators

$$M_\mu = |\text{on}\rangle \langle \text{on}| \otimes K_\mu + |\text{off}\rangle \langle \text{off}| \otimes \frac{1}{2} \mathcal{I}_{A'AB}, \quad (1)$$

where $\mu = 1, 2, 3, 4$ and the identity operator, $\mathcal{I}_{A'AB}$, acts on the composite Hilbert space consisting of Alice’s two qubits, A' and A , and Bob’s qubit, B . $\mathcal{I}_{A'AB}$ has been pre-factored with a $1/2$ so that the relation $\sum_{\mu=1}^4 M_\mu^\dagger M_\mu = \mathcal{I}_{S A'AB}$ is satisfied. The operators, M_μ , act on the composite Hilbert space consisting of the switch, S , along with A' , A , and B .

Let us assume that initially the switch’s state is in superposition of the states $|\text{on}\rangle$ and $|\text{off}\rangle$, viz. $\alpha |\text{on}\rangle + \beta |\text{off}\rangle$, where α and β are complex coefficients and $|\alpha|^2 + |\beta|^2 = 1$. Hence the joint initial state of the four qubits is given by

$$|\xi\rangle = (\alpha |\text{on}\rangle + \beta |\text{off}\rangle)_S |\psi\rangle_{A'} |\psi^-\rangle_{AB}.$$

Therefore, after going through Protocol 1, the output state will be

$$\begin{aligned} \rho_{S A'AB}^{\text{Pr}_1} &= \sum_{\mu=1}^4 M_\mu |\xi\rangle \langle \xi| M_\mu^\dagger \\ &= |\alpha|^2 |\text{on}\rangle \langle \text{on}| \otimes \sum_{\mu=1}^4 K_\mu \rho K_\mu^\dagger + \frac{\alpha\beta^*}{2} |\text{on}\rangle \langle \text{off}| \otimes \sum_{\mu=1}^4 K_\mu \rho \\ &\quad + \frac{\alpha^*\beta}{2} |\text{off}\rangle \langle \text{on}| \otimes \sum_{\mu=1}^4 \rho K_\mu^\dagger + |\beta|^2 |\text{off}\rangle \langle \text{off}| \otimes \rho. \end{aligned}$$

We now consider two separate paths in succession.

Path 1: Along the first path, we simply throw away the switch (i.e., trace it out), and get

$$\begin{aligned} \rho_{A'AB}^{\text{Pr}_1 \text{Pa}_1} &= |\alpha|^2 \sum_{\mu=1}^4 K_\mu \rho K_\mu^\dagger + |\beta|^2 \rho \\ &= |\alpha|^2 (|\psi^-\rangle \langle \psi^-|)_{A'A} (|\psi\rangle \langle \psi|)_B + |\beta|^2 \rho. \end{aligned}$$

The resulting state of Bob’s qubit is

$$\rho_B^{\text{Pr}_1 \text{Pa}_1} = \text{Tr}_{A'A} (\rho_{A'AB}^{\text{Pr}_1 \text{Pa}_1}) = |\alpha|^2 |\psi\rangle \langle \psi| + \frac{|\beta|^2}{2} \mathcal{I}_B,$$

where $\text{Tr}_{A'A}$ denotes partial trace over A' and A . This is the same state that one would have obtained if there was no switch, but Alice and Bob simply sleep away with probability $|\beta|^2$, which is exactly the “weight” of the $|\text{off}\rangle$ term in the switch’s state.

The fidelity of the output (at B) to the input (that was inserted into A' initially) is

$$\mathcal{F}_{\text{Pr}_1 \text{Pa}_1} = |\alpha|^2 + \frac{|\beta|^2}{2}.$$

From normalization condition of the switch’s state, we have $|\alpha|^2 + |\beta|^2 = 1$. Thus, we can take $\alpha = \cos(\theta/2)$ and $\beta = \exp(i\phi) \sin(\theta/2)$, with $\theta \in [0, \pi]$ and $\phi \in [0, 2\pi)$. Then, we get

$$\mathcal{F}_{\text{Pr}_1 \text{Pa}_1}(\theta) = \frac{1}{2} \left(1 + \cos^2 \frac{\theta}{2} \right). \quad (2)$$

We see that the fidelity is independent of the input state, $|\psi\rangle_{A'}$, and only depends on the switch’s initial state. Clearly, $\mathcal{F}_{\text{Pr}_1 \text{Pa}_1}$ in this case is always $\geq \frac{1}{2}$ ($\frac{1}{2}$ is the average fidelity for a random guess). Moreover, it is greater than $\frac{2}{3}$ for $\cos \frac{\theta}{2} > \frac{1}{\sqrt{3}}$, i.e., $\theta < 141.06^\circ$ ($\frac{2}{3}$ is the maximal fidelity achievable when there is classical communication between the parties but there is no shared entanglement and no switch).

Instead of a switch, if we consider the classical mixture of two situations, where with probability $|\alpha|^2$, the singlet is available, and with probability $|\beta|^2$, it is not, then the average fidelity in absence of classical communication will be $|\alpha|^2 + \frac{|\beta|^2}{2}$. Thus we see that in this case, the switch does not provide any advantage over classical mixtures. To realize the effect of “superposition” in the task, we next introduce another path.

Path 2: Let us now move to the second path. In this path, after getting the state $\sum_{\mu} M_\mu |\xi\rangle \langle \xi| M_\mu^\dagger$, we rotate the state of the switch by a Hadamard operator, H_s . H_s transforms $|\text{on}\rangle$ and $|\text{off}\rangle$ to $(|\text{on}\rangle + |\text{off}\rangle)/\sqrt{2}$ and $(|\text{on}\rangle - |\text{off}\rangle)/\sqrt{2}$ respectively. After the application of the operator, we measure the switch’s state in the $\{|\text{on}\rangle, |\text{off}\rangle\}$ basis and choose the whole output when the outcome is associated with the $|\text{on}\rangle$ state (briefly, we say this as ‘the outcome is the $|\text{on}\rangle$ state’). Note that probability of getting the $|\text{on}\rangle$ state as output is $(4 - \sin \theta \cos \phi)/8$ and the final output state following this path is given by

$$\rho_{A'AB}^{\text{Pr}_1 \text{Pa}_2} = \sum_{\mu=1}^4 \left(\frac{|\alpha|^2}{2} K_\mu \rho K_\mu^\dagger + \frac{\alpha\beta^*}{4} K_\mu \rho + \frac{\alpha^*\beta}{4} \rho K_\mu^\dagger \right) + \frac{|\beta|^2}{2} \rho.$$

But the state, $\rho_{A'AB}^{\text{Pr}_1 \text{Pa}_2}$, is not normalized. After normalizing the state and then taking trace over A and A' we can obtain the state of the qubit on Bob’s side, which is given by

$$\rho_B^{\text{Pr}_1 \text{Pa}_2} = \frac{4|\alpha|^2 - \alpha\beta^* - \beta\alpha^*}{4 - \alpha\beta^* - \beta\alpha^*} |\psi\rangle \langle \psi| + \frac{2|\beta|^2}{4 - \alpha\beta^* - \beta\alpha^*} \mathcal{I}_B.$$

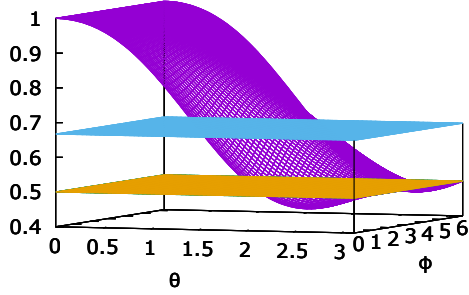


FIG. 1: Fidelity of teleported state to the actual state in Protocol 1 Path 2. We plot $\mathcal{F}_{\text{Pr}_1\text{Pa}_2}$ along the vertical axis as a function of the switch-state's parameters θ and ϕ which are represented in radians in the horizontal axes. The violet color depicts the value of $\mathcal{F}_{\text{Pr}_1\text{Pa}_2}$. The vertical axis is dimensionless. The functional form of the fidelity is expressed in Eq. (3). We present $\mathcal{F}_{\text{Pr}_1\text{Pa}_2} = \frac{1}{2}$ and $\mathcal{F}_{\text{Pr}_1\text{Pa}_2} = \frac{2}{3}$ planes using yellow and sky-blue colors respectively, to compare the fidelity of Protocol 1 Path 2 with the fidelity of random guess and with the maximum fidelity accomplished through the classical process, i.e., measure and prepare without shared entanglement.

Hence the fidelity of the state of B to the initial state of A' is given by

$$\begin{aligned}\mathcal{F}_{\text{Pr}_1\text{Pa}_2}(\theta, \phi) &= \frac{2(1 + \cos^2 \frac{\theta}{2}) - \sin \theta \cos \phi}{4 - \sin \theta \cos \phi} \\ &= \frac{3 + \cos \theta - \sin \theta \cos \phi}{4 - \sin \theta \cos \phi},\end{aligned}\quad (3)$$

which is again - like for Path 1 - independent of $|\psi\rangle_{A'}$. Instead of $|\text{on}\rangle$ state, if the output corresponding to $|\text{off}\rangle$ state is chosen, then the corresponding fidelity is given by- $\mathcal{F}'_{\text{Pr}_1\text{Pa}_2} = \frac{3 + \cos \theta + \sin \theta \cos \phi}{4 + \sin \theta \cos \phi}$. Thus, we see the fidelities corresponding to the measurement outcomes $|\text{on}\rangle$ and $|\text{off}\rangle$ are interchangeable under the transformation $\phi \rightarrow \phi + \pi$. However, unless specified, we mostly discuss about $\mathcal{F}_{\text{Pr}_1\text{Pa}_2}$.

In Fig. 1, we plot the fidelity, $\mathcal{F}_{\text{Pr}_1\text{Pa}_2}$, as a function of the switch's state's parameters, θ and ϕ . To compare it with the values $\frac{1}{2}$ and $\frac{2}{3}$, we also plot the planes $\mathcal{F}_{\text{Pr}_1\text{Pa}_2} = \frac{1}{2}$ and $\mathcal{F}_{\text{Pr}_1\text{Pa}_2} = \frac{2}{3}$ in the same figure. It can be understood from the figure, that though $\mathcal{F}_{\text{Pr}_1\text{Pa}_2}$ is not always greater than $\frac{2}{3}$ or $\frac{1}{2}$, there exists a wide range of values of θ and ϕ for which not only $\mathcal{F}_{\text{Pr}_1\text{Pa}_2} > \frac{1}{2}$ but also $\mathcal{F}_{\text{Pr}_1\text{Pa}_2} > \frac{2}{3}$. To understand precisely, the ranges of θ and ϕ , for which $\mathcal{F}_{\text{Pr}_1\text{Pa}_2} > \frac{1}{2}$ or $\mathcal{F}_{\text{Pr}_1\text{Pa}_2} > \frac{2}{3}$, in Fig. 2, we plot $\mathcal{F}_{\text{Pr}_1\text{Pa}_2} - \frac{1}{2}$ (left panel) and $\mathcal{F}_{\text{Pr}_1\text{Pa}_2} - \frac{2}{3}$ (right panel). The figure clearly indicates that though $\mathcal{F}_{\text{Pr}_1\text{Pa}_2}$ is not always greater than $\frac{2}{3}$, it is almost always greater than $\frac{1}{2}$ except for two small regions (of the (θ, ϕ) -plane).

Since Path 1 always achieves fidelity greater than $\frac{1}{2}$ (fidelity corresponding to a random guess) whereas there are instances when fidelity corresponding to Path 2 is less than $\frac{1}{2}$, one may apparently conclude that usage of the Hadamard rotation does not have any overall advantage. But this is not the case. In the following subsection, we present a formal comparison between the two paths.

Which path to follow?

We have seen that Path 1 does not provide any improvement over the scenario where classical mixture is considered instead of switch. But in case of Path 2, there exists regions of values of the switch's parameters, θ and ϕ , where Path 2 is more preferable than Path 1 implying fidelity gain over classical mixture. It can be realized by taking the difference between the fidelities of the two paths, that is

$$D_1(\theta, \phi) = \mathcal{F}_{\text{Pr}_1\text{Pa}_2} - \mathcal{F}_{\text{Pr}_1\text{Pa}_1} = \frac{\sin \theta \cos \phi (\cos \theta - 1)}{4(4 - \sin \theta \cos \phi)}. \quad (4)$$

From Eq. (4), it is clear that which path is more convenient, depends on the switch's initial state, in particular the value of ϕ . Whatever the value of θ , Path 2 will always be more beneficial for $\frac{\pi}{2} \leq \phi \leq \frac{3\pi}{2}$. But this range of ϕ will get altered to the complementary region if we choose $|\text{off}\rangle$ instead of $|\text{on}\rangle$ in Path 2. In that case, $\mathcal{F}'_{\text{Pr}_1\text{Pa}_2} - \mathcal{F}_{\text{Pr}_1\text{Pa}_1} \geq 0$ is satisfied for $\phi \leq \frac{\pi}{2}$ and $\phi \geq \frac{3\pi}{2}$. Thus, if the freedom of choosing $|\text{on}\rangle$ or $|\text{off}\rangle$, depending on the initial state of the switch (in particular, of ϕ), is provided, then the difference between the fidelities of the two paths is given by

$$D_1^{\max}(\theta, \phi) = \mathcal{F}_{\text{Pr}_1\text{Pa}_2}^{\max} - \mathcal{F}_{\text{Pr}_1\text{Pa}_1} = \left| \frac{\sin \theta \cos \phi (\cos \theta - 1)}{4(4 - \sin \theta \cos \phi)} \right|, \quad (5)$$

become always non-negative. Here we have used the notation $\mathcal{F}_{\text{Pr}_1\text{Pa}_2}^{\max} = \max\{\mathcal{F}_{\text{Pr}_1\text{Pa}_2}, \mathcal{F}'_{\text{Pr}_1\text{Pa}_2}\}$. In Fig. 5, we plot D_1^{\max} (in the left panel) as a function of θ and ϕ . Hence, we see that if we choose Path 2, Protocol 1 provides advantage, except for a set of measure zero on the (θ, ϕ) -plane, in the sense that the fidelity of teleportation is always better than when a classical mixture of the $|\text{on}\rangle$ and $|\text{off}\rangle$ states of the quantum switch is utilized.

Let us next consider the situation where classical communication is also allowed between the two parties. And then we examine how the resource improves the efficiency of the task.

IV. ROLE OF CLASSICAL COMMUNICATION

We are now going to introduce the second protocol. It's similar with the previous protocol, except that in this case, we have the facility of using classical communication when there is no singlet shared between the parties. Note that it is reasonable to do so, as when the singlet is present, the usual teleportation protocol is followed, which utilizes classical communication. Thus, in this protocol, when the singlet is not present Alice measures her qubit $|\psi\rangle_{A'}$ in an arbitrary basis

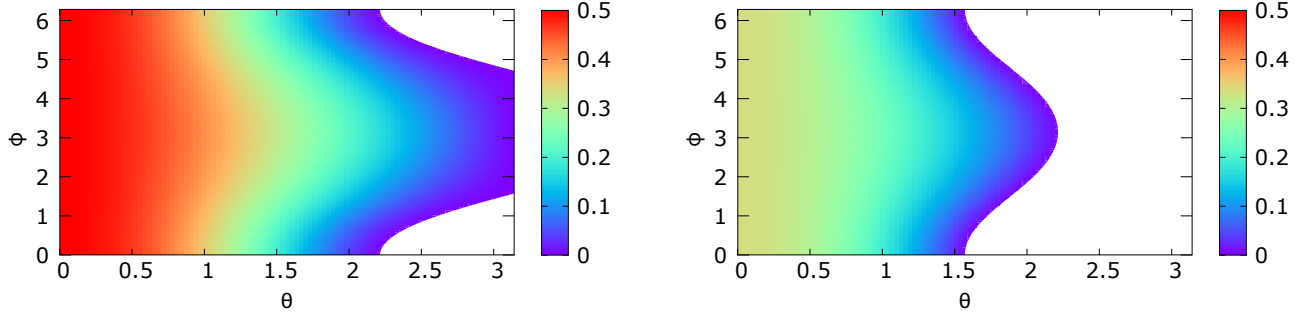


FIG. 2: Advantages of the quantum teleportation protocol over random guess and classical protocols. We plot $\mathcal{F}_{\text{Pr1Pa2}} - \frac{1}{2}$ (left panel) and $\mathcal{F}_{\text{Pr1Pa2}} - \frac{2}{3}$ (right panel) as functions of the angles θ and ϕ . The horizontal and vertical axes represent the parameters θ and ϕ respectively and are presented in radian unit. The value of the fidelity, $\mathcal{F}_{\text{Pr1Pa2}} - \frac{1}{2}$ or $\mathcal{F}_{\text{Pr1Pa2}} - \frac{2}{3}$, is indicated using color where the exact value corresponding to a particular color is demonstrated in the color box. The fidelities are dimensionless.

(say, the computational basis), sends the information about the outcome classically to Bob, and Bob throws away his part

of the singlet and prepares a qubit in a state that is same as the outcome at Alice. The corresponding transformation can mathematically be expressed as

$$((a|0\rangle + b|1\rangle)_{A'} \otimes |\psi^-\rangle_{AB})((a^* \langle 0| + b^* \langle 1|)_{A'} \otimes \langle \psi^-|_{AB}) \longrightarrow |a|^2 |0\rangle_{A'} \langle 0| \otimes \left(\frac{\mathcal{I}_A}{2}\right)_A \otimes |0\rangle_B \langle 0| + |b|^2 |1\rangle_{A'} \langle 1| \otimes \left(\frac{\mathcal{I}_A}{2}\right)_A \otimes |1\rangle_B \langle 1|,$$

where $a|0\rangle + b|1\rangle$ represents the initial state $|\psi\rangle_{A'}$. To describe this protocol, we have to replace the $\mathcal{I}_{AA'B}$ in Eq. (1) by a new set of Kraus operators, $\{L_\nu\}$, given by

$$L_1 = |000\rangle \langle 001|, L_2 = |010\rangle \langle 010|, \\ L_3 = |101\rangle \langle 101|, L_4 = |111\rangle \langle 110|.$$

It can be easily checked that $\sum_\nu L_\nu(|\psi\rangle \langle \psi|)_{A'}(|\psi^-\rangle \langle \psi^-|)_{AB} L_\nu^\dagger = |a|^2 |0\rangle_{A'} \langle 0| \otimes \left(\frac{\mathcal{I}_A}{2}\right)_A \otimes |0\rangle_B \langle 0| + |b|^2 |1\rangle_{A'} \langle 1| \otimes \left(\frac{\mathcal{I}_A}{2}\right)_A \otimes |1\rangle_B \langle 1|$. But the set of operators, $\{L_\nu\}_\nu$, does not satisfy the completeness relation, that is $\sum_{\nu=1}^4 L_\nu^\dagger L_\nu \neq \mathcal{I}_{AA'B}$. To complete the set of Kraus operators, we additionally define the four Kraus operators,

$$L_5 = |\chi_1\rangle \langle 000|, L_6 = |\chi_2\rangle \langle 011|, \\ L_7 = |\chi_3\rangle \langle 100|, L_8 = |\chi_4\rangle \langle 111|.$$

For an arbitrary normalized set of states $\{|\chi_i\rangle\}_i$, the operators satisfy $\sum_{\nu=1}^8 L_\nu^\dagger L_\nu = \mathcal{I}_{A'AB}$ and $L_\nu(|\psi\rangle \langle \psi|)_{A'}(|\psi^-\rangle \langle \psi^-|)_{AB} L_\nu^\dagger = 0$ for $\nu = 5, 6, 7, 8$.

To describe the entire process of **Protocol 2**, we define the set of Kraus operators,

$$N_{\mu\nu} = \frac{1}{\sqrt{8}} |\text{on}\rangle \langle \text{on}| \otimes K_\mu + \frac{1}{2} |\text{off}\rangle \langle \text{off}| \otimes L_\nu,$$

which acts on the composite Hilbert space consisting of S , A ,

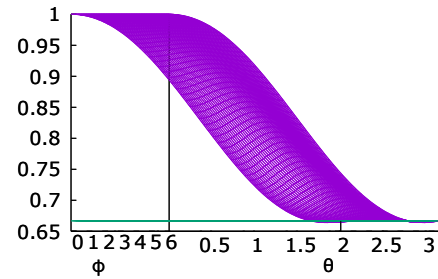


FIG. 3: Performance of the second teleportation protocol. We plot the fidelity of the output state of Bob's qubit to the actual expected state after going through Protocol 2 Path 2. $\mathcal{F}_{\text{Pr2Pa2}}$ (see Eq. (7)) is plotted along the vertical axis against θ and ϕ along the horizontal axes, using radian as the unit. The vertical axis is dimensionless. To compare the fidelity with the classical case, we also plot the plane $\frac{2}{3}$ in the same graph.

A' , and B . Hence the final output state of the protocol is

$$\rho_{SA'AB}^{\text{Pr2}} = \sum_{\mu=1}^4 \sum_{\nu=1}^8 N_{\mu\nu} |\xi\rangle \langle \xi| N_{\mu\nu}^\dagger.$$

Path 1: Recalling Path 1, we trace out the switch from $\rho_{SA'AB}^{\text{Pr2}}$

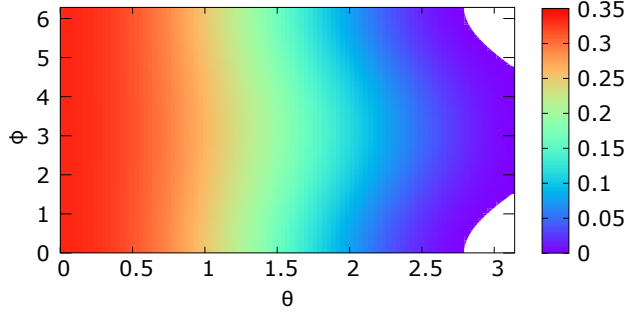


FIG. 4: Comparison between the fidelity attained using Protocol 2 Path 2 and the maximum attainable fidelity using classical method. All considerations here are the same as in the right panel of Fig. 2, except the fact that here we have considered Protocol 2, and thus, instead of plotting $\mathcal{F}_{\text{Pr}_1\text{Pa}_2} - \frac{2}{3}$, we plot $\mathcal{F}_{\text{Pr}_2\text{Pa}_2} - \frac{2}{3}$.

and get

$$\rho_{A'AB}^{\text{Pr}_2\text{Pa}_1} = |\alpha|^2 \sum_{\mu=1}^4 K_{\mu} \rho K_{\mu}^{\dagger} + |\beta|^2 \sum_{\nu=1}^8 L_{\nu} \rho L_{\nu}^{\dagger}.$$

Now if we ignore the qubits A and A' , the state of B is given by

$$\rho_B^{\text{Pr}_2\text{Pa}_1} = |\alpha|^2 |\psi\rangle\langle\psi| + |\beta|^2 (|a|^2 |0\rangle\langle 0| + |b|^2 |1\rangle\langle 1|).$$

$$\rho_{A'AB}^{\text{Pr}_2\text{Pa}_2} = \frac{|\alpha|^2}{2} \sum_{\mu=1}^4 K_{\mu} \rho K_{\mu}^{\dagger} + \frac{\alpha\beta^*}{4\sqrt{8}} \left(\sum_{\mu=1}^4 K_{\mu} \right) \rho \left(\sum_{\nu=1}^8 L_{\nu}^{\dagger} \right) + \frac{\alpha^*\beta}{4\sqrt{8}} \left(\sum_{\nu=1}^8 L_{\nu} \right) \rho \left(\sum_{\mu=1}^4 K_{\mu}^{\dagger} \right) + \frac{|\beta|^2}{2} \sum_{\nu=1}^8 L_{\nu} \rho L_{\nu}^{\dagger}.$$

The above state is not normalized. After normalizing and tracing out A' and A , we are left with Bob's system described by the following state:

$$\begin{aligned} \rho_B^{\text{Pr}_2\text{Pa}_2} = & \frac{16|\alpha|^2 - \sqrt{2}(\alpha^*\beta + \beta^*\alpha)}{16 - \sqrt{2}(\alpha^*\beta + \beta^*\alpha)} |\psi\rangle\langle\psi| \\ & + \frac{16|\beta|^2}{16 - \sqrt{2}(\alpha^*\beta + \beta^*\alpha)} [|a|^2 |0\rangle\langle 0| + |b|^2 |1\rangle\langle 1|]. \end{aligned}$$

Fidelity of the state, $\rho_B^{\text{Pr}_2\text{Pa}_2}$, to the expected state $|\psi\rangle\langle\psi|$ is

$$F_2 = \frac{16|\alpha|^2 - \sqrt{2}(\alpha^*\beta + \beta^*\alpha) + 16|\beta|^2(|a|^4 + |b|^4)}{16 - \sqrt{2}(\alpha^*\beta + \beta^*\alpha)}.$$

Hence the average fidelity, with the average being taken over

Fidelity of the above output state, to the desired initial state, $|\psi\rangle\langle\psi|$ is

$$F_1 = |\alpha|^2 + |\beta|^2(|a|^4 + |b|^4) = |\alpha|^2 + |\beta|^2 \left(\cos^4 \frac{\theta'}{2} + \sin^4 \frac{\theta'}{2} \right).$$

Here we have set $a = \cos(\theta'/2)$ and $b = e^{i\phi'} \sin(\theta'/2)$, where $\theta' \in [0, \pi]$ and $\phi' \in [0, 2\pi]$. Since the fidelity, F_1 , depends on the initial state of the qubit A' , to have an overall idea about the success of the protocol, we take average of F_1 over the complete set of input states. We get

$$\begin{aligned} \mathcal{F}_{\text{Pr}_2\text{Pa}_1}(\theta, \phi) &= \frac{1}{4\pi} \int_0^{2\pi} \int_0^{\pi} F_1 \sin \theta' d\theta' d\phi' = |\alpha|^2 + \frac{2}{3} |\beta|^2 \\ &= \cos^2 \frac{\theta}{2} + \frac{2}{3} \sin^2 \frac{\theta}{2} = \frac{1}{3} \left(2 + \cos^2 \frac{\theta}{2} \right). \end{aligned} \quad (6)$$

Hence, the average fidelity in this case is $\geq \frac{2}{3}$ for all θ and ϕ .

Again, if we consider the situation where the availability of the singlet depends on a probability distribution, i.e., with $|\alpha|^2$ probability the singlet is present and with probability $|\beta|^2$ it is not, the corresponding average fidelity will be exactly equal to $\mathcal{F}_{\text{Pr}_2\text{Pa}_1}$. Therefore, in the following part, we follow the second path in the hope of gaining quantum advantage.

Path 2: If we follow the second path, we have to apply the Hadamard gate on the switch's state and measure the switch in the basis $\{| \text{on} \rangle, | \text{off} \rangle\}$. The state corresponding to the output $| \text{on} \rangle$ will be

all possible initial pure states of A' , is given by

$$\begin{aligned} \mathcal{F}_{\text{Pr}_2\text{Pa}_2}(\theta, \phi) &= \frac{48|\alpha|^2 - 3\sqrt{2}(\alpha^*\beta + \beta^*\alpha) + 32|\beta|^2}{48 - 3\sqrt{2}(\alpha^*\beta + \beta^*\alpha)}, \\ &= \frac{40 + 8\cos\theta - 3\sqrt{2}\sin\theta\cos\phi}{48 - 3\sqrt{2}\sin\theta\cos\phi}. \end{aligned} \quad (7)$$

It is easy to check that the above fidelity is greater than $\frac{1}{2}$. In Fig. 3, we plot $\mathcal{F}_{\text{Pr}_2\text{Pa}_2}$ with respect to θ and ϕ . To compare it with the maximum classical fidelity, we also plot the plane with a height of $\frac{2}{3}$, in the same figure. As it can be noticed from the figure, there exists a very small region where $\mathcal{F}_{\text{Pr}_2\text{Pa}_2}$ is less than $\frac{2}{3}$. This is also evident from Fig. 4, where we exhibit a projected plot of $\mathcal{F}_{\text{Pr}_2\text{Pa}_2} - \frac{2}{3}$.

We have observed that Path 1 of the second protocol mimics the classical mixture scenario in terms of fidelity, $\mathcal{F}_{\text{Pr}_2\text{Pa}_1}$, of the output state. To obtain quantum advantage, one has to follow the second path. In the following subsection, we dis-

cuss about the difference between the effectivenesses of the two paths and regions of the parameter space where Path 2 is more advantageous than Path 1.

Comparison between the two paths

The difference between the two average fidelities corresponding to the two paths of Protocol 2 is given by

$$D_2(\theta, \phi) = \mathcal{F}_{\text{Pr}_2\text{Pa}_2} - \mathcal{F}_{\text{Pr}_2\text{Pa}_1} = \frac{\sin \theta \cos \phi (\cos \theta - 1)}{\sqrt{2} (48 - 3\sqrt{2} \sin \theta \cos \phi)}. \quad (8)$$

It is evident from the Eq. (8) that $D_2(\theta, \phi) \geq 0$ for $\frac{\pi}{2} \leq \phi \leq \frac{3\pi}{2}$, i.e., in this region, quantum advantage can be achieved by following Path 2.

If we consider the scenario where the measurement output $|\text{off}\rangle$ has been chosen instead of $|\text{on}\rangle$ in Path 2, the corresponding fidelity of Bob's state would be $\mathcal{F}'_{\text{Pr}_2\text{Pa}_2}(\theta, \phi) = \frac{40+8\cos\theta+3\sqrt{2}\sin\theta\cos\phi}{48+3\sqrt{2}\sin\theta\cos\phi}$, i.e., $\mathcal{F}'_{\text{Pr}_2\text{Pa}_2}(\theta, \phi) = \mathcal{F}_{\text{Pr}_2\text{Pa}_2}(\theta, \phi + \pi)$. By choosing between $\mathcal{F}_{\text{Pr}_2\text{Pa}_2}$ and $\mathcal{F}'_{\text{Pr}_2\text{Pa}_2}$, we can cover the full range of ϕ such that the second path becomes more profitable, by providing quantum advantage. In Fig. 5, we plot

$$D_2^{\max} = \max\{\mathcal{F}'_{\text{Pr}_2\text{Pa}_2}, \mathcal{F}_{\text{Pr}_2\text{Pa}_2}\} - \mathcal{F}_{\text{Pr}_2\text{Pa}_1} \quad (9)$$

in the right panel as a function of θ and ϕ . From the figure it is evident that the distinction between the fidelities of the two paths in Protocol 1 is much more intense than in Protocol 2.

V. QUANTUM ADVANTAGE AND QUANTUM COHERENCE OF SWITCH'S STATE

From Eqs. (4) and (8), it is clear that the advantage of following one path over the other depends on the switch's initial state, in particular, the value of α and β . Since the initial state of switch, $|\alpha|^2 |\text{on}\rangle\langle\text{on}| + |\beta|^2 |\text{off}\rangle\langle\text{off}|$, would not have given any quantum advantage (when the reference basis is $\{|\text{on}\rangle, |\text{off}\rangle\}$), we expect that the resource behind the quantum advantage is provided by the superposition in the switch's initial state. Therefore, we want to explore the relation between the quantum coherence of the switch's state, which is a quantifier of superposition, and the advantage of the second path over the first one, in the context of the two protocols individually.

The l_1 -norm of quantum coherence, C , of a state, say σ , in an arbitrary but fixed basis $\{|i\rangle\}_i$, is given by [55–57]

$$C(\sigma) = \sum_{i,j,i \neq j} |\langle i|\sigma|j\rangle|.$$

Thus, we see that the quantum coherence of a state is a basis-dependent quantity.

The initial state of the switch is considered to be $\alpha |\text{on}\rangle + \beta |\text{off}\rangle$. We assume that $\{|\text{on}\rangle, |\text{off}\rangle\}$ are eigenstates corresponding to the Pauli matrix σ_z . Therefore, the quantum coherence

of the switch state in σ_z basis, i.e., with respect to $\{|\text{on}\rangle, |\text{off}\rangle\}$, is

$$c_z = |\alpha^*\beta| + |\alpha\beta^*| = \sin \theta,$$

whereas the coherence in σ_x basis, i.e., with respect to $\left\{\frac{|\text{on}\rangle+|\text{off}\rangle}{\sqrt{2}}, \frac{|\text{on}\rangle-|\text{off}\rangle}{\sqrt{2}}\right\}$, is given by

$$\begin{aligned} c_x &= \frac{1}{2} (|\cos \theta + i \sin \theta \sin \phi| + |\cos \theta - i \sin \theta \sin \phi|) \\ &= \sqrt{1 - \sin^2 \theta \cos^2 \phi}. \end{aligned}$$

The difference between the two fidelities of Protocol 1 can be expressed in terms of the coherence, c_z , in the following way:

$$\begin{aligned} \Delta_1(c_z, \phi) &= \frac{c_z \cos \phi \left(\sqrt{1 - c_z^2} - 1 \right)}{4(4 - c_z \cos \phi)} \text{ for } 0 \leq \theta \leq \frac{\pi}{2}, \\ &= -\frac{c_z \cos \phi \left(\sqrt{1 - c_z^2} + 1 \right)}{4(4 - c_z \cos \phi)} \text{ for } \frac{\pi}{2} \leq \theta \leq \pi. \end{aligned}$$

Let us first focus on the first range, i.e., $0 \leq \theta \leq \frac{\pi}{2}$. The corresponding function, $\Delta_1(c_z, \phi)$, is clearly positive in the range $\frac{\pi}{2} \leq \phi \leq \frac{3\pi}{2}$. It implies that within this range, the operation of the Hadamard gate and measurement in the switch's basis provide advantage over Path 1.

The derivative of $\Delta_1(c_z, \phi)$ with respect to c_z is given by

$$\begin{aligned} \frac{\partial \Delta_1(c_z, \phi)}{\partial c_z} &= \frac{\cos \phi \left(4 - 4\sqrt{1 - c_z^2} - 8c_z^2 + c_z^3 \cos \phi \right)}{4(4 - c_z \cos \phi)^2 \sqrt{1 - c_z^2}} \\ &\text{for } 0 \leq \theta \leq \frac{\pi}{2}. \end{aligned}$$

It can be easily checked that the function $4 - 4\sqrt{1 - c_z^2} - 8c_z^2 + c_z^3 \cos \phi$ has maximum at $c_z = 0$ and the corresponding maximum value is 0. Moreover, since $c_z \geq 0$ and $\cos \phi \leq 0$ for $\frac{\pi}{2} \leq \phi \leq \frac{3\pi}{2}$, $4 - 4\sqrt{1 - c_z^2} - 8c_z^2 + c_z^3 \cos \phi \leq c_z^3 \cos \phi \leq 0$, which implies $\frac{\partial \Delta_1(c_z, \phi)}{\partial c_z} \geq 0$. Hence, we conclude within the range $0 \leq \theta \leq \frac{\pi}{2}$ when $\Delta_1(c_z, \phi)$ is positive, the function is a monotonically increasing function of c_z , that is, the advantage of using Hadamard gate increases with the coherence in the initial switch's state.

Let us now move to the second range, i.e., $\frac{\pi}{2} \leq \theta \leq \pi$. It is surely negative within the range $\phi \leq \frac{\pi}{2}$ or $\phi \geq \frac{3\pi}{2}$ and positive for $\frac{\pi}{2} \leq \phi \leq \frac{3\pi}{2}$. Since we want to examine the situation where the second path is advantageous, we are interested in the second region. The derivative of the function, $\Delta_1(c_z, \phi)$, with respect to c_z is given by

$$\begin{aligned} \frac{\partial \Delta_1(c_z, \phi)}{\partial c_z} &= -\frac{\cos \phi \left(4 + 4\sqrt{1 - c_z^2} - 8c_z^2 + c_z^3 \cos \phi \right)}{4(4 - c_z \cos \phi)^2 \sqrt{1 - c_z^2}} \\ &\text{for } \frac{\pi}{2} \leq \theta \leq \pi. \end{aligned}$$

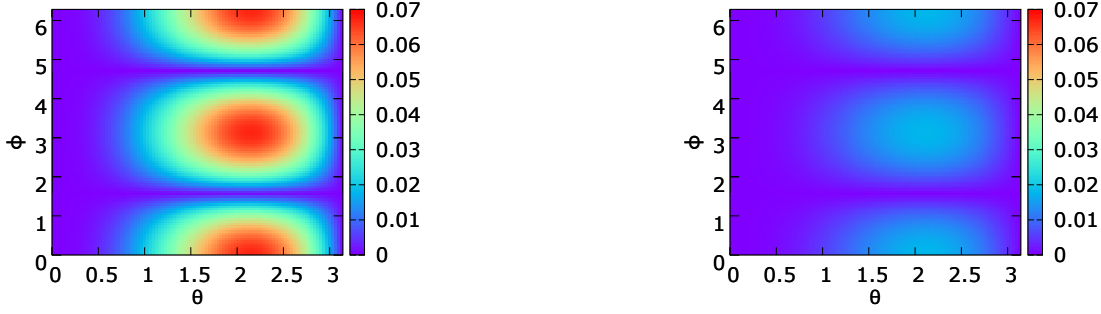


FIG. 5: Variation between the two paths of the teleportation protocols. We plot the difference between the maximum fidelity corresponding to Path 2 (maximized over fidelities corresponding to the two scenarios, i.e., choosing $|\text{on}\rangle$ or $|\text{off}\rangle$, as a preferable measurement outcome) and the fidelity for following Path 1, by performing Protocol 1 (left panel) and Protocol 2 (right panel). In particular, we plot $\mathcal{F}_{\text{Pr1Pa2}} - \mathcal{F}_{\text{Pr1Pa1}}$ and $\mathcal{F}_{\text{Pr2Pa2}} - \mathcal{F}_{\text{Pr2Pa1}}$ as functions of θ (horizontal axis) and ϕ (vertical axis). The angles θ and ϕ are considered in radian unit. The functional forms are expressed in Eqs. (5) and (9). The fidelities are dimensionless.

The above function can be both positive and negative, depending on the particular values of c_z and ϕ . For example, $\frac{\partial \Delta_1(0, \pi)}{\partial c_z} = 0.125 > 0$ and $\frac{\partial \Delta_1(0.9, \pi)}{\partial c_z} = -0.035 < 0$. Therefore, in this range, the quantum coherence of switch cannot guarantee the increasing advantage of Path 2. We have expressed the difference between the two fidelities, i.e., $D_1(\theta, \phi)$ or $\Delta_1(c_z, \phi)$, in terms of the quantum coherences c_z and c_x in the Appendix.

Let us now move to Protocol 2 where classical communication is allowed even when the switch is in the $|\text{off}\rangle$ state. The difference between the two fidelities in this protocol can also be written in terms of the coherence c_z and can be expressed as

$$\Delta_2(c_z, \phi) = \frac{c_z \cos \phi \left(\sqrt{1 - c_z^2} - 1 \right)}{\sqrt{2} (48 - 3 \sqrt{2} c_z \cos \phi)} \text{ for } 0 \leq \theta \leq \frac{\pi}{2},$$

$$= -\frac{c_z \cos \phi \left(\sqrt{1 - c_z^2} + 1 \right)}{\sqrt{2} (48 - 3 \sqrt{2} c_z \cos \phi)} \text{ for } \frac{\pi}{2} \leq \theta \leq \pi.$$

Considering each range separately and following the same path of logic and calculations as in the previous one, we obtain the following points:

1. Within the range $0 \leq \theta \leq \frac{\pi}{2}$ and $\phi \leq \frac{\pi}{2}$ or $\phi \geq \frac{3\pi}{2}$, Path 1 is more preferable than Path 2.
2. Path 2 is beneficial within the range $0 \leq \theta \leq \frac{\pi}{2}$, $\frac{\pi}{2} \leq \phi \leq \frac{3\pi}{2}$. Moreover, the amount of advantage of using Path 2 is a monotonically increasing function of the quantum coherence, c_z .
3. In the range $\frac{\pi}{2} \leq \theta \leq \pi$ and $\phi \leq \frac{\pi}{2}$ or $\phi \geq \frac{3\pi}{2}$, again Path 1 will attain more fidelity than Path 2.
4. In the remaining region, i.e., $\frac{\pi}{2} \leq \theta \leq \pi$ and $\frac{\pi}{2} \leq \phi \leq \frac{3\pi}{2}$, though Path 2 is more advantageous, increasing quantum coherence may not help to raise the advantage.

As we have discussed earlier in detail, the above points are also true for Protocol 1.

The difference in the fidelities of Protocol 2, $D_2(\theta, \phi)$ or $\Delta_2(c_z, \phi)$, can be represented as a function of the two coherences, c_z and c_x . One can go through the Appendix for the exact expressions.

VI. CONCLUSION

Perfect teleportation of a quantum state to a distant location needs a maximally entangled state to be shared between the sender and the receiver. If the shared state is entangled but not maximally entangled, then the teleported state may not be perfect but it may have fidelity more than the maximum fidelity achievable by using classical communication only.

We considered a scenario where Alice (the sender) and Bob (the receiver) are using a set-up that is in a superposition of situations of sharing a maximally entangled state and of not having any shared state. The protocol is controlled by a quantum switch. When Alice and Bob share a maximally entangled state, and in this case, the switch is “on”, the usual teleportation protocol is performed. Otherwise, when the switch is “off”, they either do nothing (Protocol 1) or Alice measures her system in an arbitrary basis, classically informs Bob about her output, and Bob prepares a system in that output state (Protocol 2). So, they make use of classical communication as a resource in Protocol 2, while the same resource is absent in Protocol 1. For each of the two protocols, we use two paths: in the first path, after accomplishing the usual teleportation protocol, we simply throw away the switch, and in the second path, instead of throwing away the switch, we apply a rotation on the switch’s state, measure it, and consider the output corresponding to a particular state. We compare the average fidelity of the output state to the initial target state with the average fidelity of a random guess and with the maximum average fidelity using the “classical method”. We see that Proto-

col 1 Path 1 gives a fidelity that is always greater than random guess whereas the Protocol 2 Path 1 gives fidelity greater than the classical method. This is intuitively satisfactory, since in Protocol 2 we have used classical communication, as for the classical method.

An obvious question arises here: which path is better? We see for both protocols, the answer depends only on the phase of the superposition and not on the probability amplitudes. We examine if there exists any relation between the advantage of the second path over the first path and quantum coherence in the switch's initial state. The connection between the quantum coherence and the difference between the fidelities depends on the range of the parameters defining the superposition of $|\text{on}\rangle$ and $|\text{off}\rangle$ states of the quantum switch. For example, for a particular range, the difference is a monotonically increasing function of the quantum coherence.

ACKNOWLEDGMENTS

The research of KS was supported in part by the INFOSYS scholarship. SH was supported by a postdoctoral fellowship of Harish-Chandra Research Institute, Prayagraj (Allahabad) when part of this work was completed. SH is now supported by the "Quantum Optical Technologies" project, carried out within the International Research Agendas program of the Foundation for Polish Science cofinanced by the European Union under the European Regional Development Fund. We acknowledge partial support from the Department of Science and Technology, Government of India through the QuEST grant (grant number DST/ICPS/QUST/Theme3/2019/120).

APPENDIX

The difference between the two fidelities of Protocol 1, i.e $D_1(\theta, \phi)$ or $\Delta_1(c_z, \phi)$, can be expressed in terms of the coherences c_z and c_x . The functional form depends on the range of θ and ϕ . Considering the four distinct ranges of the parameters individually, we have presented the functional forms of $\mathcal{G}_1(c_z, c_x) = \mathcal{F}_{\text{Pr1Pa2}} - \mathcal{F}_{\text{Pr1Pa1}}$ in the following way: (i) For $0 \leq \theta \leq \frac{\pi}{2}$ and $\phi \leq \frac{\pi}{2}$ or $\phi \geq \frac{3\pi}{2}$,

$$\mathcal{G}_1(c_z, c_x) = \frac{\sqrt{1-c_x^2} \left(\sqrt{1-c_z^2} - 1 \right)}{4 \left(4 - \sqrt{1-c_x^2} \right)}.$$

(ii) For $0 \leq \theta \leq \frac{\pi}{2}$ and $\frac{\pi}{2} \leq \phi \leq \frac{3\pi}{2}$,

$$\mathcal{G}_1(c_z, c_x) = -\frac{\sqrt{1-c_x^2} \left(\sqrt{1-c_z^2} - 1 \right)}{4 \left(4 + \sqrt{1-c_x^2} \right)}.$$

(iii) For $\frac{\pi}{2} \leq \theta \leq \pi$ and $\phi \leq \frac{\pi}{2}$ or $\phi \geq \frac{3\pi}{2}$,

$$\mathcal{G}_1(c_z, c_x) = -\frac{\sqrt{1-c_x^2} \left(\sqrt{1-c_z^2} + 1 \right)}{4 \left(4 - \sqrt{1-c_x^2} \right)}.$$

(iv) For $\frac{\pi}{2} \leq \theta \leq \pi$ and $\frac{\pi}{2} \leq \phi \leq \frac{3\pi}{2}$,

$$\mathcal{G}_1(c_z, c_x) = \frac{\sqrt{1-c_x^2} \left(\sqrt{1-c_z^2} + 1 \right)}{4 \left(4 + \sqrt{1-c_x^2} \right)}.$$

The difference in the fidelities of Protocol 2, $D_2(\theta, \phi)$ or $\Delta_2(c_z, \phi)$, can also be represented as a function of the two coherences, c_z and c_x in the following way: (i) For $0 \leq \theta \leq \frac{\pi}{2}$ and $\phi \leq \frac{\pi}{2}$ or $\phi \geq \frac{3\pi}{2}$,

$$\mathcal{G}_2(c_z, c_x) = \frac{\sqrt{1-c_x^2} \left(\sqrt{1-c_z^2} - 1 \right)}{\sqrt{2} \left(48 - 3\sqrt{2}\sqrt{1-c_x^2} \right)}.$$

(ii) For $0 \leq \theta \leq \frac{\pi}{2}$ and $\frac{\pi}{2} \leq \phi \leq \frac{3\pi}{2}$,

$$\mathcal{G}_2(c_z, c_x) = -\frac{\sqrt{1-c_x^2} \left(\sqrt{1-c_z^2} - 1 \right)}{\sqrt{2} \left(48 + 3\sqrt{2}\sqrt{1-c_x^2} \right)}.$$

(iii) For $\frac{\pi}{2} \leq \theta \leq \pi$ and $\phi \leq \frac{\pi}{2}$ or $\phi \geq \frac{3\pi}{2}$,

$$\mathcal{G}_2(c_z, c_x) = -\frac{\sqrt{1-c_x^2} \left(\sqrt{1-c_z^2} + 1 \right)}{\sqrt{2} \left(48 - 3\sqrt{2}\sqrt{1-c_x^2} \right)}.$$

(iv) For $\frac{\pi}{2} \leq \theta \leq \pi$ and $\frac{\pi}{2} \leq \phi \leq \frac{3\pi}{2}$,

$$\mathcal{G}_2(c_z, c_x) = \frac{\sqrt{1-c_x^2} \left(\sqrt{1-c_z^2} + 1 \right)}{\sqrt{2} \left(48 + 3\sqrt{2}\sqrt{1-c_x^2} \right)}.$$

[1] C. H. Bennett, G. Brassard, C. Crepeau, R. Jozsa, A. Peres, and W. Wootters, Teleporting an unknown quantum state via dual classical and Einstein-Podolsky-Rosen channels, *Phys. Rev. Lett.* **70**, 1895 (1993).

[2] S. Pirandola, J. Eisert, C. Weedbrook, A. Furusawa, and S. L. Braunstein, Advances in quantum teleportation, *Nat. Photonics* **9**, 641 (2015).

[3] H.-J. Briegel, W. Dür, J. I. Cirac, and P. Zoller, Quantum re-

- peaters: The role of imperfect local operations in quantum communication, *Phys. Rev. Lett.* **81**, 5932 (1998).
- [4] D. Gottesman and I. L. Chuang, Demonstrating the viability of universal quantum computation using teleportation and single-qubit operations, *Nature* **402**, 390 (1999).
 - [5] M. Żukowski, A. Zeilinger, M. A. Horne, and A. K. Ekert, “Event-ready-detectors” Bell experiment via entanglement swapping, *Phys. Rev. Lett.* **71**, 4287 (1993).
 - [6] M. Żukowski, A. Zeilinger, and H. Weinfurter, Entangling photons radiated by independent pulsed sources, *Ann. N.Y. Acad. Sci.* **755**, 91 (1995).
 - [7] S. Bose, V. Vedral, and P.L. Knight, Multiparticle generalization of entanglement swapping, *Phys. Rev. A* **57**, 822 (1998).
 - [8] S. Bose, V. Vedral, and P.L. Knight, Purification via entanglement swapping and conserved entanglement, *Phys. Rev. A* **60**, 194 (1999).
 - [9] C. H. Bennett, D. P. DiVincenzo, P. W. Shor, J. A. Smolin, B. M. Terhal, and W. K. Wootters, Remote state preparation, *Phys. Rev. Lett.* **87**, 077902 (2001).
 - [10] M. Muraio, D. Jonathan, M. B. Plenio, and V. Vedral, Quantum telecloning and multiparticle entanglement, *Phys. Rev. A* **59**, 156 (1999).
 - [11] D. Bouwmeester, J.-W. Pan, K. Mattle, M. Eibl, H. Weinfurter, and A. Zeilinger, Experimental quantum teleportation, *Nature* **390**, 575 (1997).
 - [12] I. Marcikic, H. de Riedmatten, W. Tittel, H. Zbinden, and N. Gisin, Long-distance teleportation of qubits at telecommunication wavelengths, *Nature* **421**, 509 (2003).
 - [13] R. Ursin, T. Jennewein, M. Aspelmeyer, R. Kaltenbaek, M. Lindenthal, P. Walther, and A. Zeilinger, Quantum teleportation across the Danube, *Nature* **430**, 849 (2004).
 - [14] Jin, X.-M., et al. Experimental free-space quantum teleportation, *Nature Photonics* **4**, 376 (2010).
 - [15] X.-S. Ma, T. Herbst, T. Scheidl, D. Wang, S. Kropatschek, W. Naylor, B. Wittmann, A. Mech, J. Kofler, E. Anisimova, V. Makarov, T. Jennewein, R. Ursin, and A. Zeilinger, Quantum teleportation over 143 kilometres using active feed-forward, *Nature* **489**, 269 (2012).
 - [16] J. Yin, et al., Quantum teleportation and entanglement distribution over 100-kilometre free-space channels, *Nature* **488**, 185 (2012).
 - [17] M. D. Barrett, J. Chiaverini, T. Schaetz, J. Britton, W. M. Itano, J. D. Jost, E. Knill, C. Langer, D. Leibfried, R. Ozeri, and D. J. Wineland, Deterministic quantum teleportation of atomic qubits, *Nature* **429**, 737 (2004).
 - [18] M. Riebe, H. Häffner, C. F. Roos, W. Hänsel, J. Benhelm, G. P. T. Lancaster, T. W. Körber, C. Becher, F. Schmidt-Kaler, D. F. V. James, and R. Blatt., Deterministic quantum teleportation with atoms, *Nature* **429**, 734 (2004).
 - [19] M. A. Nielsen, E. Knill, and R. Laflamme, Complete quantum teleportation using nuclear magnetic resonance, *Nature* **396**, 52 (1998).
 - [20] L. Steffen, Y. Salathe, M. Oppliger, P. Kurpiers, M. Baur, C. Lang, C. Eichler, G. Puebla-Hellmann, A. Fedorov, and A. Wallraff, Deterministic quantum teleportation with feed-forward in a solid state system, *Nature* **500**, 319 (2013).
 - [21] I. Marcikic, H. de Riedmatten, W. Tittel, H. Zbinden, and N. Gisin, Long distance quantum teleportation of qubits from photons at 1300 nm to photons at 1550 nm wavelength, *Nature* **421**, 509 (2003).
 - [22] S. Takeda, T. Mizuta, M. Fuwa, P. v. Loock, and A. Furusawa, Deterministic quantum teleportation of photonic quantum bits by a hybrid technique, *Nature* **500**, 315 (2013).
 - [23] F. Bussières, C. Clausen, A. Tiranov, B. Kozh, V. B. Verma, S. W. Nam, F. Marsili, A. Ferrier, P. Goldner, H. Herrmann, C. Silberhorn, W. Sohler, M. Afzelius, and N. Gisin, Quantum teleportation from a telecom-wavelength photon to a solid-state quantum memory, *Nature Photonics* **8**, 775 (2014).
 - [24] R. Horodecki, M. Horodecki, and P. Horodecki, Teleportation, Bell’s inequalities and inseparability, *Phys. Lett. A* **222**, 21 (1996).
 - [25] R. Jozsa, Fidelity for mixed quantum states, *J. Mod. Opt.* **41**, 2315 (2007).
 - [26] N. Gisin, Nonlocality criteria for quantum teleportation, *Phys. Lett. A* **210**, 157 (1996).
 - [27] M. Horodecki, P. Horodecki, and R. Horodecki, General teleportation channel, singlet fraction, and quasidistillation, *Phys. Rev. A* **60**, 1888 (1999).
 - [28] G. Bowen and S. Bose, Teleportation as a depolarizing quantum channel, relative entropy, and classical capacity, *Phys. Rev. Lett.* **87**, 267901 (2001).
 - [29] D. Cavalcanti, P. Skrzypczyk, and I. Šupić, All entangled states can demonstrate non-classical teleportation, *Phys. Rev. Lett.* **119**, 110501 (2017).
 - [30] J. Bang, J. Ryu, and D. Kaszlikowski, Fidelity deviation in quantum teleportation, *J. Phys. A: Math. Theor.* **51**, 135302 (2018).
 - [31] G. Carvacho, F. Andreoli, L. Santodonato, M. Bentivegna, V. D’Ambrosio, P. Skrzypczyk, I. Šupić, D. Cavalcanti, and F. Sciarrino, Experimental study of nonclassical teleportation beyond average fidelity, *Phys. Rev. Lett.* **121**, 140501 (2018).
 - [32] S. Popescu, Bell’s inequalities versus teleportation: What is nonlocality?, *Phys. Rev. Lett.* **72**, 797 (1994).
 - [33] S. Massar and S. Popescu, Optimal extraction of information from finite quantum ensembles, *Phys. Rev. Lett.* **74**, 1259 (1995).
 - [34] G. Chiribella, G. M. D’Ariano, P. Perinotti, and B. Valiron, Quantum computations without definite causal structure, *Phys. Rev. A* **88**, 022318 (2013).
 - [35] M. Araújo, F. Costa, and C. Brukner, Computational advantage from quantum-controlled ordering of gates, *Phys. Rev. Lett.* **113**, 250402 (2014).
 - [36] C. Brukner, Quantum causality, *Nat. Phys.* **10**, 259 (2014).
 - [37] M. Araújo, C. Branciard, F. Costa, A. Feix, C. Giarmatzi, and C. Brukner, Witnessing causal nonseparability, *New J. Phys.* **17**, 102001 (2015).
 - [38] D. Ebler, S. Salek, and G. Chiribella, Enhanced communication with the assistance of indefinite causal order, *Phys. Rev. Lett.* **120**, 120502 (2018).
 - [39] S. Salek, D. Ebler, and G. Chiribella, Quantum communication in a superposition of causal orders, arXiv:1809.06655.
 - [40] O. Oreshkov, Time-delocalized quantum subsystems and operations: on the existence of processes with indefinite causal structure in quantum mechanics, *Quantum* **3**, 206 (2019).
 - [41] X. Zhao, Y. Yang, and G. Chiribella, Quantum metrology with indefinite causal order, *Phys. Rev. Lett.* **124**, 190503 (2020).
 - [42] C. Mukhopadhyay and A. K. Pati, Superposition of causal order enables perfect quantum teleportation with very noisy singlets, *J. Phys. Commun.* **4**, 105003 (2020).
 - [43] G. Chiribella, M. Banik, S. S. Bhattacharya, T. Guha, M. Alimuddin, A. Roy, S. Saha, S. Agrawal, and G. Kar, Indefinite causal order enables perfect quantum communication with zero capacity channels, *New Journal of Physics* **23**, 033039 (2021).
 - [44] P. R. Dieguez, V. F. Lisboa, and R. M. Serra, Thermal devices powered by generalized measurements with indefinite causal order, arxiv:2205.14406.
 - [45] P. A. Guérin, A. Feix, M. Araújo, and C. Brukner, Exponential communication complexity advantage from quantum superposition of the direction of communication, *Phys. Rev. Lett.* **117**,

- 100502 (2016).
- [46] L. M. Procopio, A. Moqanaki, M. Araujo, F. Costa, I. A. Calafell, E. G. Dowd, D. R. Hamel, L. A. Rozema, C. Brukner, and P. Walther, Experimental superposition of orders of quantum gates, *Nature Communications* **6**, 7913 (2015).
 - [47] G. Rubino, L. A. Rozema, A. Feix, M. Araújo, J. M. Zeuner, L. M. Procopio, C. Brukner, and P. Walther, Experimental verification of an indefinite causal order, *Sci. Adv.* **3**, e1602589 (2017).
 - [48] K. Goswami, C. Giarmatzi, M. Kewming, F. Costa, C. Branciard, J. Romero, and A. G. White, Indefinite causal order in a quantum switch, *Phys. Rev. Lett.* **121**, 090503 (2018).
 - [49] M. M. Taddei, J. Cariñe, D. Martínez, T. García, N. Guerrero, A. A. Abbott, M. Araújo, C. Branciard, E. S. Gómez, S. P. Walborn, L. Aolita, and G. Lima, Computational advantage from the quantum superposition of multiple temporal orders of photonic gates, *PRX Quantum* **2**, 010320 (2021).
 - [50] G. Rubino, L. A. Rozema, F. Massa, M. Araújo, M. Zych, Č. Brukner, and P. Walther, Experimental entanglement of temporal order, *Quantum* **6**, 621 (2022).
 - [51] R. Jozsa, Quantum effects in algorithms, arXiv: quant-ph/9805086.
 - [52] M. A. Siddiqui and T. Qureshi, Multipath wave-particle duality with a path detector in a quantum superposition, *Phys. Rev. A* **103**, 022219 (2021).
 - [53] J. Zhang, C. Xie, and K. Peng, Quantum switch for continuous variable teleportation, *J. Opt. B: Quantum Semiclass. Opt.* **3**, 293 (2001).
 - [54] M. Caleffi and A. S. Cacciapuoti, Quantum switch for the quantum internet: noiseless communications through noisy channels, *IEEE Journal on Selected Areas in Communications* **38**, 575 (2020).
 - [55] T. Baumgratz, M. Cramer, and M. B. Plenio, Quantifying Coherence, *Phys. Rev. Lett.* **113**, 140401 (2014).
 - [56] K. Bu and C. Xiong, A note on cohering power and de-cohering power, *Quant. Inf. Comp.* **17**, 1206 (2017).
 - [57] S. Rana, P. Parashar, and M. Lewenstein, Trace-distance measure of coherence, *Phys. Rev. A* **93**, 012110 (2016).